Original Article

Fe₃O₄@Ag Nanoprobe for Detection of Ovarian Cancer Cell Line Using Magnetic Resonance Imaging

Shiva Aghaei[1,2]M.Sc., Seyedhossein Hekmatimoghaddam[2,3]M.D.
Mehdi Kalantar[1]Ph.D., Mohammad Hassan Sheikha[1]M.D., Ph.D.
Mohammad Sobhan[4]M.D., Ali Jebali[2,3*]Ph.D.

[1]Department of Genetics, Faculty of Medicine, Shahid Sadoughi University of Medical Sciences, Yazd, Iran.
[2]Department of Advanced Medical Sciences and Technologies, Faculty of Paramedicine, Shahid Sadoughi University of Medical Sciences, Yazd, Iran.
[3]Department of Laboratory Sciences, Faculty of Paramedicine, Shahid Sadoughi University of Medical Sciences, Yazd, Iran.
[4]Department of Radiology, Faculty of Medicine, Shahid Sadoughi University of Medical Sciences, Yazd, Iran.

A B S T R A C T

Background and Aims: Magnetic resonance imaging (MRI) plays an essential role in molecular imaging by delivering the contrast agent into targeted cells. The aim of this study was to evaluate the use of magnetic nanoparticles containing iron oxide and silver (Fe₃O₄@Ag core-shell nanoprobe) as a contrast agent for the detection of ovarian cancer cell line ovcar-3.

Materials and Methods: Co-precipitation method was used for synthesis of Fe₃O₄Ag nanoprobe which was then characterized by Fourier transform infrared spectroscopy (FTIR), dynamic light scattering (DLS) and scanning electron microscope (SEM). To evaluate the ability of this nanoprobe in detection of the ovcar-3 cell line by MRI, the cells were exposed to different (5 to 50 μg/mL) concentrations of Fe₃O₄@Ag nanoprobe before contrast intensity calculation by MRI.

Results: SEM images revealed that Fe₃O₄@Ag nanoparticles are spherical, about 100 nm. FTIR showed strong absorbance picks belonging to the stretching vibration of Ag and Fe-O. It was found that contrast intensity of Fe₃O₄@Ag nanoprobe decreases as concentration decreases. Statistical analysis revealed significant difference in concentrations of 30, 40 and 50 μg/mL, compared to control ($p < 0.05$). In the presence of Ovcar-3 cells, higher concentrations (10, 20, and 30 μg/mL) of nanoparticles also significantly increased contrast intensity in comparison with control ($p < 0.05$).

Conclusions: This novel magnetic nanoparticle can be used as an effective contrast agent for improving MRI in detection of ovarian cancer cells. The sensitivity of this contrast agent may be improved by binding to targeting molecules such as antibody and aptamer.

*Corresponding Author: Department of Laboratory Sciences, Faculty of Paramedicine, Shahid Sadoughi University of Medical Sciences, Yazd, Iran. **Tel:** +989900152139, **Email:** alijebal2011@gmail.com

Introduction

In spite of remarkable investment in research on cancer, it is still the second most common cause of death (25 percent of deaths in the developed countries) [1]. Early diagnosis and treatment of cancer can provide significantly higher chances of survival. However, current diagnostic techniques can hardly detect half of patients with cancer at an early stage [2]. Despite recent advancements in conventional diagnostic modalities, we are still behind confident detections regarding sensitivity and specificity factors [3]. More than 60% of patients with breast, lung, colon and ovarian cancer have hidden or metastatic colonies at diagnosis [4]. The second most common cancer of the female genital system is ovarian cancer which carries a higher mortality rate than all other gynecologic malignancies [5].

Doppler ultrasonography (US), computed tomography (CT), and magnetic resonance imaging (MRI) are the most common imaging methods used to detect ovarian cancer. They enjoy high accuracy in diagnosis of malignancy. Comparison of these methods has shown that MRI has the highest sensitivity and accuracy [6-9]. Although several imaging methods are available, none of them has both sensitivity and accuracy required to diagnose ovarian cancer in early stages [10]. Currently, only about 25% of carcinomas of the ovary can be detected in the early stages. Therefore, finding more efficient methods to improve the conventional diagnostics can significantly improve the survival rate of the patients [11-13]. Due to high significance of contrast agents in MRI, several studies are currently under way to introduce new contrast agents such as magnetic nanoparticles. Magnetic iron oxide (MIO) has long blood retention time, biodegradability and low toxicity. It is one of the primary nanomaterials for biomedical applications. MIO plays a vital role as an MRI contrast agent. Generally, superparamagnetic iron oxide (SPIO) can be detected at micromolar concentrations and can provide sufficient sensitivity [14-16]. Moreover, magnetic nanoprobes (MNPs) have exciting possibilities in monitoring response to treatment. The unique physical properties of NPs has nominated them as excellent candidates for application of biological interactions at cellular and molecular levels [16, 17].

In this study, a new formulation of magnetic nanoparticles containing iron oxide and silver was constructed and characterized. The final formulation can be shown by $Fe_3O_4@Ag$. Then, human ovarian cancer cells (cell line Ovcar-3) were exposed to them and imaged by MRI.

Materials and Methods

Human ovarian cancer cell line (Ovcar-3) was purchased from the Pasteur Institute in Tehran, Iran. All of the chemicals were of analytical grade and purchased from commercial sources. $FeCl_2.4H_2O$, $FeCl_3.6H_2O$, NaOH, and $AgNO_3$ were obtained from Merck, Germany. Streptomycin, penicillin G and phosphate buffer (20 mM, pH=7.8) were purchased from Sigma,

International Journal of Medical Laboratory 2018;5(2): 123-132.

124

Germany. Fetal bovine serum (FBS) and Dulbecco's Modified Eagle's Medium (DMEM) as a culture medium and other supplements were obtained from Gibco, USA.

Synthesis of Fe₃O₄@Ag nanoprobe

As is seen in figure 1, 1M of $FeCl_2.4H_2o$ and 1M of $FeCl_3.6H_2o$ were prepared and stirred at room temperature. Then, serial concentrations of NaOH ($1-10^{-3}$ M) were added drop-wisely to serial concentrations of $FeCl_2:FeCl_3$ ($1-10^{-3}$ M) at room temperature. Fe_3O_4 nanoparticles were separated using an external magnetic field, and washed with deionized water. Then, NaOH (1 M) was added to precipitated nanoparticles, and serial concentrations of $AgNo_3$ were added. Later, they were washed with deionized water and added (100 mg/mL) to the $Fe_3O_4@Ag$ pellet before stir for 1h at room temperature.

After magnetic separation, the nanoprobe was washed three times using phosphate buffered saline (PBS) (pH 7.4) to remove the unbound fraction. Finally, the nanoprobe was resuspended in 1 mL PBS buffer (pH 7.4) and stored at 4 °C [18, 19]. The morphology of $Fe_3O_4@Ag$ nanoprobe was observed using scanning electron microscope (SEM) (Hitachi S-4800 II, Japan). The IR spectra were taken using Nicolet Magna 550 Fourier transform infrared spectroscopy (FTIR) (USA) by applying spectroscopic-grade KBr. The size and zeta potential of NPs were assessed by dynamic light scattering (DLS) (Nano-ZS 90, Malvern Instrument, United Kingdom). Also, the contrast image of final nanoparticle was measured by MRI apparatus (M13, USA).
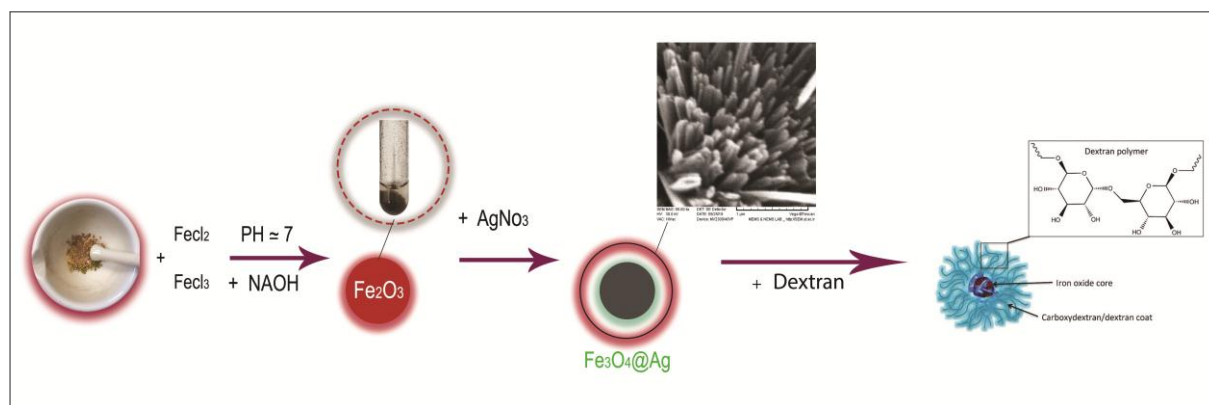

Fig. 1. Schematic procedure of [Fe₃O₄@Ag] nanoprobe synthesis

Cell culture

Ovcar-3 cells are adapted with DMEM and RPMI culture media. In this research, they were grown in DMEM medium supplemented with 10% heat-inactivated FBS, penicillin (100 U/mL), and streptomycin (100 µg/mL) at 37°C in humidified atmosphere with 5% CO_2. The cells were separated using 0.1% trypsin and 10 µM ethylenediaminetetraacetic acid in PBS [20].

Intervention and MRI imaging

About 10,000 cells per well were seeded into 96-well plate, and incubated for 24 h in a humidified incubator with a CO_2 concentration of 5%. Then, different concentrations of $Fe_3O_4@Ag$ nanoprobe (5 µg/mL to 30 µg/mL)

were added to the incubated cells. After 4 h, the medium was replaced with a fresh medium. Then, 96-well plate containing different concentrations of nanoprobe was imaged by MRI apparatus. In the next step, total color of each well was calculated (Total color=√R2+G2+B2) [21]. Gd++ ion at concentration of 50, 30 μg/mL was used as positive control.

Statistical analysis

All tests were performed three times, and results were reported as mean±standard deviation (SD). To detect significant differences between the groups, one-way ANOVA method was used. For this purpose, SPSS software (SPSS 16 Inc., Chicago, IL, USA) was applied, and p values less than 0.05 were considered as statistically significant. This study was approved by the Ethics Committee of Shahid Sadoughi University of medical sciences, Yazd, Iran.

Results

Characterization

Scanning electron microscope (SEM) was used to determine the size and morphology of the prepared $Fe_3O_4@Ag$ nanoprobe. Figure 2 shows that the nanoparticles have a spherical morphology with size of about 100 nm. Figure 3 shows that the mean size of the synthesized [$Fe_3O_4@Ag$] NPs was 142.9 nm by DLS technique. The zeta potential of [$Fe_3O_{4@}Ag$] nanoprobe was near -34.5 mv.
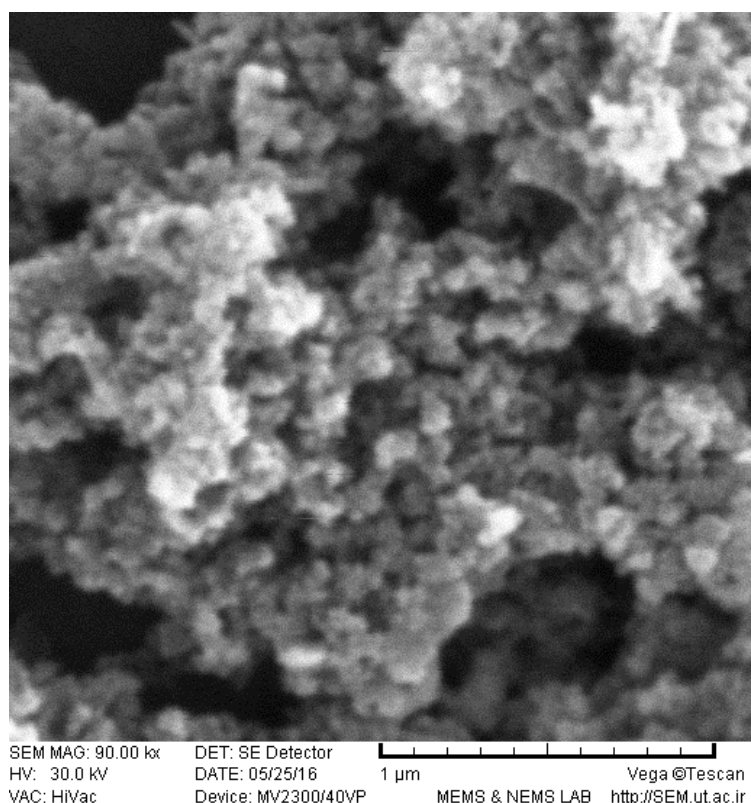

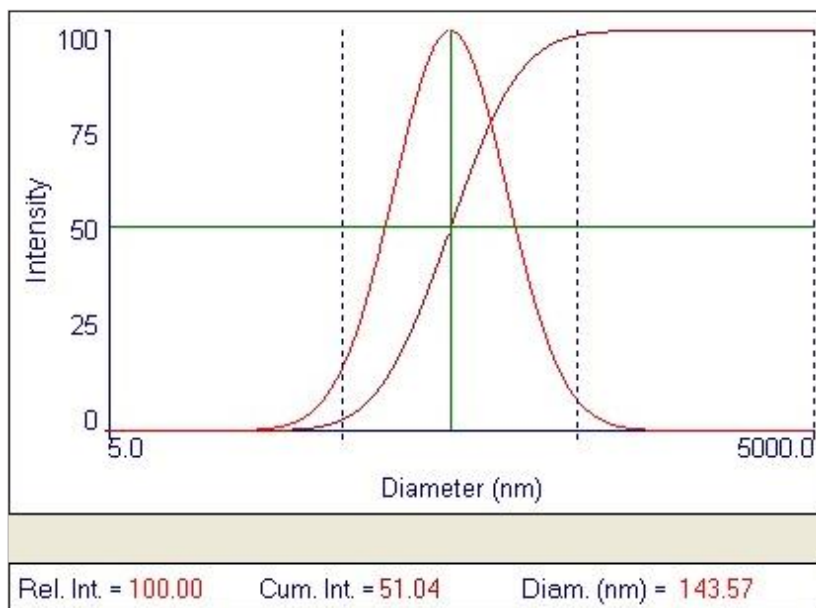**Fig. 2.** The SEM image of [$Fe_3O_4@Ag$] nanoprobe.

Fig. 3. DLS graph of [Fe₃O₄@Ag] nanoprobe. The mean size of the synthesized [Fe₃O₄@Au] NPs was 142.9 nm

FTIR was used to investigate the presence of Ag and Fe in the NPs. FTIR spectrum is presented in Figure 4 which confirms the existence of Ag and Fe in the [Fe₃O₄@Ag] NPs. In the spectrum of [Fe₃O₄@Ag] NPs, there are four strong absorbance picks at 3425, 2927, 1631, and 1431 cm⁻¹, which belong to the stretching vibration. In addition, two other absorption peaks at 586 and 540 cm⁻¹ belong to the deformation vibration of Ag and Fe-O.
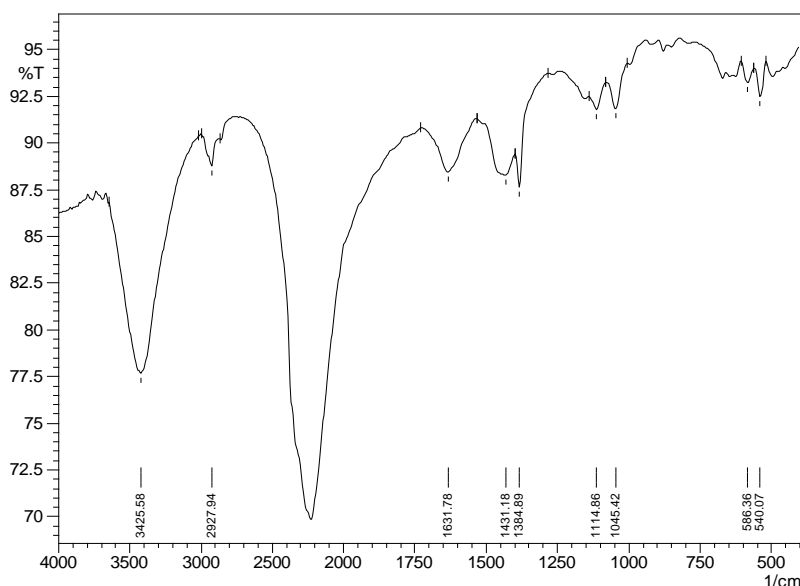

Fig. 4. The FTIR spectra of [Fe₃O₄@Ag] NPs. There are four strong absorbance picks at 3425, 2927, 1631, and 1431 cm⁻¹, which belong to the stretching vibration, while the other two absorption peaks at 586 and 540 cm⁻¹ belong to the deformation vibration of Ag and Fe-O.

MRI images

In order to investigate the utility of different concentrations of [Fe$_3$O$_4$@Ag] NP as a contrast agent, they were imaged by MRI. Figure 5a shows T$_1$-weighted MRI images of serial concentrations of Fe$_3$O$_4$@Ag nanoprobe. Figure 5b illustrates MRI contrast intensity of different concentrations of [Fe$_3$O$_4$@Ag] nanoprobe obtained by total color formula. It is clear that contrast intensity decreases as concentration is reduced. The results demonstrated that at concentration of 50 μg/mL, the contrast intensity is the highest. Statistical analysis revealed that for concentrations of 30, 40, and 50 μg/mL,

there is a significant difference compared to the control (p<0.05).

Figure 6a displays T$_1$-weighted images of ovcar-3 cells after 4 h incubation with [Fe$_3$O$_4$@Ag] nanoprobe at different concentrations. Figure 6b illustrates MRI contrast intensity of Ovcar-3 cells after 4 h incubation with [Fe$_3$O$_4$@Ag] nanoprobe at different concentrations obtained by total color formula. As shown in Figure 5, the contrast intensity has increased as the concentration increases. There were significant differences between concentrations of 10, 20, and 30 μg/mL compared to the control (p<0.05).
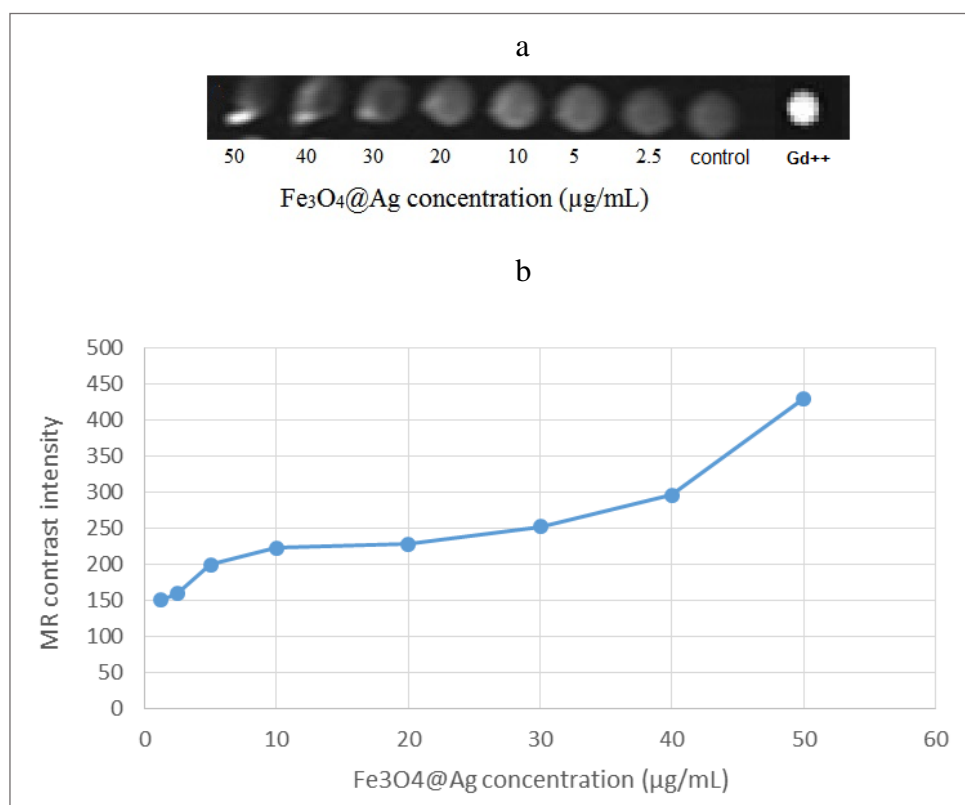

Fig. 5. MRI image of [Fe$_3$O$_4$@Ag]NPs in different concentrations (**a**). MRI contrast intensity as a contrast agent obtained by total color formula (**b**). For concentration of 30, 40, and 50 μg/mL, there was significant difference compared to control (P < 0.05). Gd++ was used as positive control.
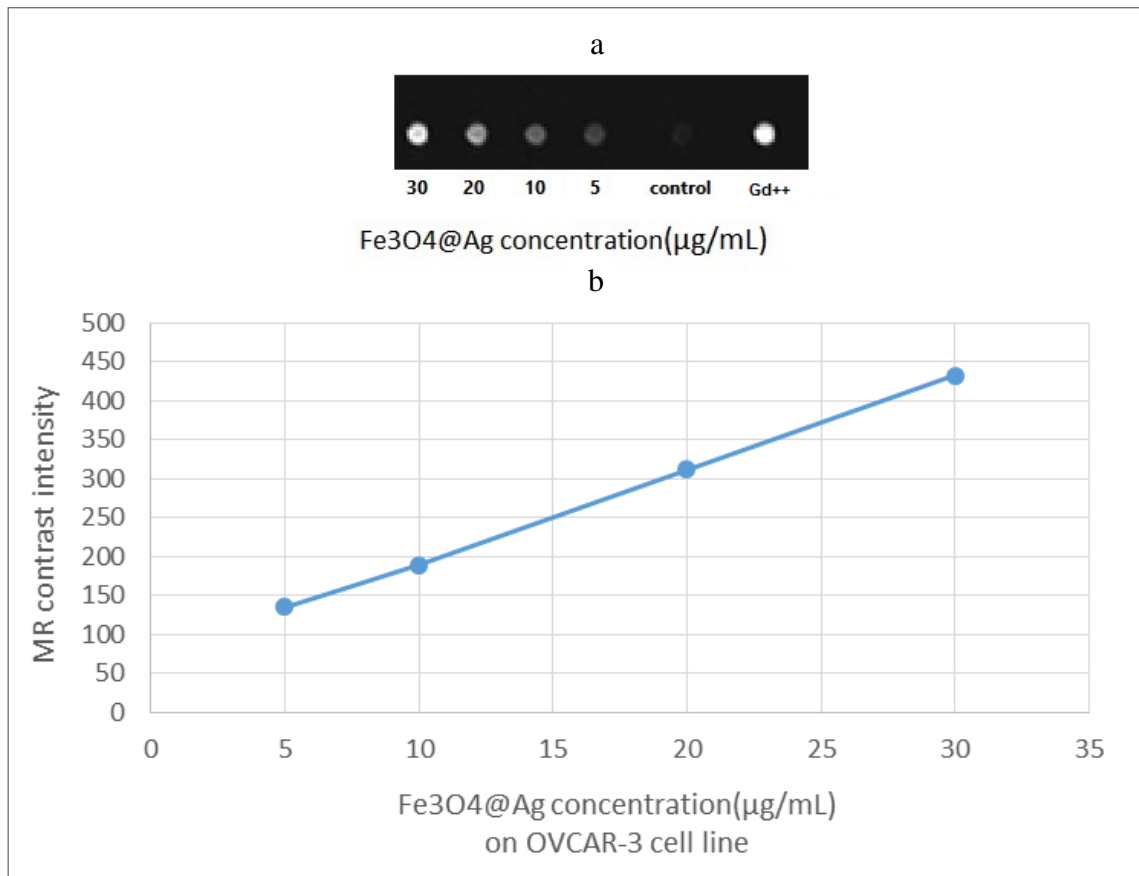
Fig. 6. T1-weighted imaging of Ovcar-3 cells after 4 h incubation with [Fe$_3$O$_4$@Ag] nanoprobe at different concentrations (a). MRI contrast intensity as a function of NPs concentration for Ovcar-3 cell treated with Fe$_3$O$_4$@Ag nanoprobe (b). There were significant differences between concentrations of 10, 20, and 30 μg/mL vs. control (P < 0.05). Gd++ was used as positive control.

Discussion

In this research, a novel nanomagnetic iron/silver (Fe$_3$O$_4$@Ag) core-shell was designed, synthesized, and characterized by FTIR, DLS and SEM. The results revealed that the nanoparticles are negatively-charged 100 nm spheres. Theoretically, these specifications make it suitable for diagnosing epithelial ovarian cancer cells by MRI. Further analysis confirmed its high contrast intensity in MRI. MNPs could be synthesized by several methods such as co-precipitation, thermal decomposition, sol-gel reaction, sono chemical, and polyol methods. They can be modified with biocompatible coatings as well as targeting

and therapeutic molecules. In this study, the co-precipitation method was used to synthesize Fe$_3$O$_4$@Ag. Here, they were simply dispersed in PBS, which can be due to dextran coating. It must be noted that some precipitation of particles was observed after 24 h. In this study, its ability to detect Ovcar-3 cells was assessed with the MRI technique. The results showed that the new formulation of magnetic nanoparticle acts as a contrast agent. This phenomenon was seen for both naked Fe$_3$O$_4$@Ag and Fe$_3$O$_4$@Ag/Ovcar-3. It was found that this nanoprobe produces bright T1-weighted MRI images at different

concentrations. The results also demonstrated that [Fe$_3$O$_4$@Ag] nanoprobe, at concentration of 50 µg/mL, has the best contrast intensity. Interestingly, contrast intensity decreased as concentration decreased. There were significant differences between concentrations of 30, 40, 50 µg/mL as compared with the control (p<0.05). Also, contrast intensity increased as the concentration increased. There were significant differences between concentration of 10, 20, and 30 µg/mL in the case vs. the control group (p<0.05).

Yang et al. developed new targeted iron oxide nanoparticles using a recombinant peptide containing amino-terminal fragment of urokinase-type plasminogen activator (uPA) conjugated with magnetic iron oxide nanoparticles (ATF-IO). That nanoprobe targets uPA receptor, which is overexpressed in breast cancer cells. Results of the MRI study showed strong contrast by a 3T MRI scanner. Their results suggested that ATF-IO nanoparticles have potential to target breast cancer [22]. Rasaneh et al. modified magnetic nanoparticles with Trastuzumab antibody to act as a new contrast agent for breast cancer. Signal intensity of SKBr3, a type of breast cancer cell line by T$_2$-weighted MRI indicated high-signal intensity compared to the control [23]. Chen et al. investigated targeted Herceptin-iron oxide nanoparticles for noninvasive imaging of HER2/neu receptors using MRI. They found that Herceptin-nanoparticles were well-dispersed in solutions of various pH range, and had no hysteresis, high saturation magnetization (80 emu/g), and low cytotoxicity to a variety of cells. Notably, the magnetic resonance

enhancements for the different breast cancer cell lines (BT-474, SKBR-3, MDA-MB-231, and MCF-7) were proportional to the HER2/neu expression level in vitro. When Herceptin-nanoparticles were administered to mice bearing breast tumor allograft by intravenous injection, the tumor site was detected in T2-weighted magnetic resonance images as a 45% enhancement drop, indicating a high level of accumulation of the contrast agent within the tumor sites [24]. Unterweger et al. worked on non-immunogenic-coated superparamagnetic iron oxide nanoparticles. It was a biocompatible, size-tunable contrast agent for MRI. To address concerns associated with hypersensitivity reactions to injectable nanoparticulate agents, they analyzed complement activation-related pseudoallergy (CARPA) upon intravenous administration of SPIONdex in a pig model. In vitro, SPIONdex did not induce hemolysis, complement or platelet activation, plasma coagulation, or leukocyte procoagulant activity, and had no relevant effect on endothelial cell viability or endothelial-monocytic cell interactions. Furthermore, SPIONdex did not induce CARPA even upon intravenous administration of 5 mg Fe/kg in pigs. Their findings suggest that due to their excellent biocompatibility, safety upon intravenous administration and size-tunability, SPIONdex particles may represent a suitable candidate for a new-generation of MRI contrast agents [25].

Our findings suggest that Fe$_3$O$_4$@Ag nanoprobe may be a promising MRI contrast agent offering the possibility of sequential imaging for early detection of ovarian cancer.

However, the acceptance of the clinical radiologists will be decisive to validate the diagnostic and prognostic value of the new iron oxide-based contrast agents in clinical trials and to ensure their broader and more efficient implementation in standard practice.

Conclusions

In this study, a novel magnetic nanoparticle was synthesized and successfully employed as an effective contrast agent for improving MRI in the detection of ovarian cancer cells. The MRI showed that the concentration of Fe$_3$O$_4$Ag nanoprobe is proportional with the image contrast intensity. So, we suggest Fe$_3$O$_4$Ag nanoprobe as a new candidate for future studies on accurate localization of cancer cells. The sensitivity of this contrast agent may be improved by binding it to targeting molecules such as antibody and aptamer.

Conflict of interest
There is no conflict of interest to declare.

Acknowledgment

References

[1]. Chinen AB, Guan CM, Ferrer JR, Barnaby SN, Merkel TJ, Mirkin CA. Nanoparticle probes for the detection of cancer biomarkers, cells, and tissues by fluorescence. Chem Rev. 2015; 115(19): 10530-10574.

[2]. A G N. The importance of early diagnosis in cancer. Can Med Assoc J. 1933; 28(5): 540-41.

[3]. Schiffman JD, Fisher PG, Gibbs P. Early detection of cancer: past, present, and future. Am Soc Clin Oncol Educ Book 2015: 57-65.

[4]. Wulfkuhle JD, Liotta LA, Petricoin EF. Proteomic applications for the early detection of cancer. Nature reviews Cancer 2003; 3(4): 267-75.

[5]. Prat J. Pathology of cancers of the female genital tract. Int J Gynaecol Obstet. 2012; 119(S 2): S137-50.

[6]. Sohaib SAA, Reznek RH. MR imaging in ovarian cancer. Cancer Imag. 2007; 7(Special issue A): S119-S29.

[7]. Mohaghegh P, Rockall AG. Imaging strategy for early ovarian cancer: characterization of adnexal masses with conventional and advanced imaging techniques. Radio Graphics 2012; 32(6): 1751-773.

[8]. Qayyum A, Coakley FV, Westphalen AC, Hricak H, Okuno WT, Powell B. Role of CT and MR imaging in predicting optimal cytoreduction of newly diagnosed primary epithelial ovarian cancer. Gynecol Oncol. 2005; 96(2): 301-306.

[9]. Kurtz AB, Tsimikas JV, Tempany CMC, Hamper UM, Arger PH, Bree RL, et al. Diagnosis and staging of ovarian cancer: comparative values of doppler and conventional US, CT, and MR imaging correlated with surgery and histopathologic analysis-report of the radiology diagnostic oncology group. Radiology 1999; 212(1): 19-27.

[10]. van Nagell JR Jr, Hoff JT. Transvaginal ultrasonography in ovarian cancer screening: current perspectives. Int J Womens Health. 2013; 6: 25-33.

[11]. Chen Y, Zhang L, Hao Q. Candidate microRNA biomarkers in human epithelial ovarian cancer: systematic review profiling studies and experimental validation. Cancer Cell Int. 2013; 13(1): 86.

[12]. Su Z, Graybill WS, Zhu Y. Detection and monitoring of ovarian cancer. Clin Chim Acta. 2013; 415: 341-45.

[13]. Badgwell D, Bast RC Jr. Early detection of ovarian cancer. Disease Markers 2007; 23(5-6): 397-410.

[14]. Bulte JWM, Kraitchman DL. Iron oxide MR contrast agents for molecular and cellular imaging. NMR Biomed. 2004; 17(7): 484-99.

[15]. Peng XH, Qian X, Mao H, Wang AY, Chen Z, Nie S, et al. Targeted magnetic iron oxide nanoparticles for tumor imaging and therapy. Int J Nanomedicine. 2008; 3(3): 311-21.

[16]. Yigit MV, Moore A, Medarova Z. Magnetic nanoparticles for cancer diagnosis and therapy. Pharmaceutic Res. 2012; 29(5): 1180-188.

[17]. Song G, Chen M, Zhang Y, Cui L, Qu H, Zheng X, et al. Janus iron oxides @

131

International Journal of Medical Laboratory 2018;5(2):123-132.

semiconducting polymer nanoparticle tracer for cell tracking by magnetic particle imaging. Nano Lett. 2018; 18(1): 182-89.

[18]. Kheiri Manjili H, Ma'mani L, Tavaddod S, Mashhadikhan M, Shafiee A, Naderi-Manesh H. D, L-Sulforaphane loaded Fe3o4@ gold core shell nanoparticles: a potential sulforaphane delivery system. PLoS One 2016; 11(3): e0151344.

[19]. Salehizadeh H, Hekmatian E, Sadeghi M, Kennedy K. Synthesis and characterization of core-shell Fe3O4-gold-chitosan nanostructure. J Nanobiotechnol. 2012; 10(1): 3.

[20]. Hernandez L, Kim MK, Lyle LT, Bunch KP, House CD, Ning F, et al. Characterization of ovarian cancer cell lines as in vivo models for preclinical studies. Gynecol Oncol. 2016; 142(2): 332-40.

[21]. Keshtkar M, Shahbazi-Gahrouei D, Khoshfetrat SM, Mehrgardi MA, Aghaei M. Aptamer-conjugated magnetic nanoparticles as targeted magnetic resonance imaging contrast agent for breast cancer. J Med Signals Sens. 2016; 6(4): 243-47.

[22]. Yang L, Peng XH, Wang YA, Wang X, Cao Z, Ni C, et al. Receptor-targeted nanoparticles for in vivo imaging of breast cancer. Clin Cancer Res. 2009; 15(14): 4722-732.

[23]. Rasaneh S, Rajabi H, Babaei MH, Akhlaghpoor S. MRI contrast agent for molecular imaging of the HER2/neu receptor using targeted magnetic nanoparticles. J Nanoparticle Res. 2011; 13(6): 2285-293.

[24]. Chen TJ, Cheng TH, Chen CY, Hsu SC, Cheng TL, Liu GC, et al. Targeted herceptin-dextran iron oxide nanoparticles for noninvasive imaging of HER2/neu receptors using MRI. J Biol Inorg Chem. 2009; 14(2): 253-60.

[25]. Unterweger H, Janko C, Schwarz M, Dézsi L, Urbanics R, Matuszak J, et al. Non-immunogenic dextran-coated superpara-magnetic iron oxide nanoparticles: A biocompatible, size-tunable contrast agent for magnetic resonance imaging. Int J Nanomedicine. 2017; 12: 5223-238.